International Journal for Numerical Methods in Engineering,
vol. 39, pp. 3163-3174 (1996)

ANISOTROPIC SMOOTHING AND SOLUTION ADAPTION FOR UNSTRUCTURED GRIDS

AHMED KHAMAYSEH AND ANDREW KUPRAT
Los Alamos National Laboratory
Los Alamos, New Mexico 87545, U.S.A.

SUMMARY

An elliptic smoothing scheme for 2-D structured meshes is generalized to the case of 2-D unstructured meshes. The resulting scheme is similar to the familiar Laplacian smoothing scheme, but exhibits superior node diffusion in anisotropic domains. We then show further improvement of grid quality when smoothing is alternated with Lawson flipping (a technique commonly used to generate Delaunay triangulations). Two additional enhancements ("controlled" and "adaptive" smoothing) allow us to create grids suitable for a realistic MOSFET semiconductor application.

Key words: anisotropic domains, quasiconformal mapping, elliptic smoothing, unstructured grids, Delaunay triangulation, adaptive smoothing, adaptive refinement.

1. INTRODUCTION

In the structured mesh community, smoothing schemes have been developed to a high degree for the production of high quality quadrilateral meshes.[1,2] In contrast, smoothing in the unstructured world of mainly triangular meshes is considerably less developed. One major problem is the absence of global curvilinear coordinates on these meshes. With structured meshes, one can easily construct a conformal or quasiconformal mapping between a logical (ξ, η)-space and the physical (x, y)-space. With unstructured meshes the situation is confused by the irregularity of the topological connectivity, leading to no such obvious mapping.

In the intermediate case of a *regular* triangular mesh, Winslow was able to find global curvilinear coordinates, and constructed a smoothing scheme by requiring the coordinates to each satisfy Laplace's equation.[3] Far from boundaries, this scheme tends towards making the position of each node equal to the average position of its neighbours. Subsequently, researchers in need of a smoothing algorithm for fully unstructured meshes have continued with the idea of replacing a node by the average position of its neighbours (even though no obvious global mapping exists to justify this process), and this has come to be known as Laplacian smoothing for unstructured grids.

One well known problem with this is that near boundaries, Laplacian smoothing can produce node spillover (where the scheme "ejects" nodes, producing triangles with negative

areas). Another problem that we have observed is poor node diffusion in anisotropic domains. Unweighted node position averaging is inherently isotropic; in this paper we will introduce weights (depending on distances between nodes) that make the scheme anisotropic and more appropriate for anisotropic domains.

Indeed, we view Laplacian smoothing for unstructured grids as a generalization of a conformal mapping smoothing scheme for structured grids. Conformal maps are angle-preserving and isotropic. Using a *quasi*-conformal mapping (a generalization of a conformal mapping which is also angle-preserving but not necessarily isotropic), we derive a new smoothing scheme which we call Elliptic Smoothing for Unstructured Grids (ESUG). In an example, we show superior diffusion of a source of points into an anisotropic domain.

In light of the extreme mobility of points under ESUG, we then develop *controlled* ESUG which limits node mobility to a user-desired degree, for those cases where complete node diffusion is not desired. Also developed is a solution adaption capability in which the mesh smoothing algorithm is modified to move grid points into areas where an objective function has large gradients. We present some real-world applications of these algorithms to MOSFET semiconductor modeling at the end of this paper.

2. ELLIPTIC SMOOTHING FOR A 2D STRUCTURED MESH

Elliptic systems have been widely recognized among the structured grid generation community to be an efficient tools to construct high quality meshes.[1] In 2D a robust elliptic system can be based on the quasiconformal mapping equations[2] to produce smooth, adaptive, orthogonal coordinates. Solution of these equations constitutes an elliptic smoothing scheme for these kinds of meshes. Here we review this scheme for structured quadrilateral meshes; this scheme will be generalized to unstructured meshes in the following section.

We assume that the boundary nodes in our quadrilateral mesh are fixed, but we are free to move interior nodes. It is desired that interior node positions be adjusted to achieve a smooth variation in quadrilateral shape and area given the constraints on the boundary nodes. Now consider a quasiconformal mapping $\varphi = \xi(x,y) + i\eta(x,y)$ from the region D in (x,y)-space to a region R in (ξ,η)-space, Figure 1.

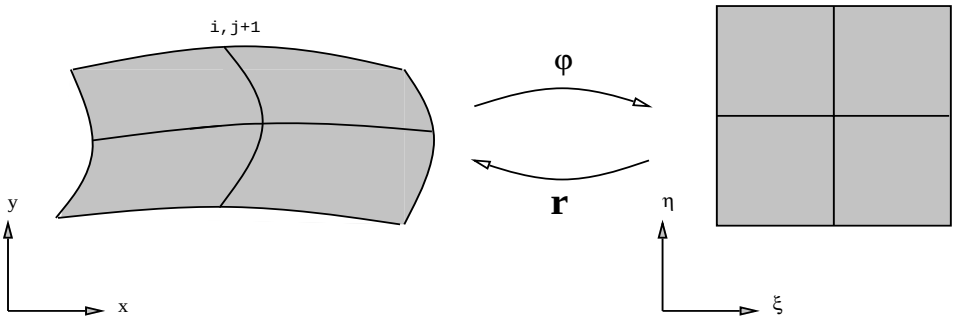

By definition, the real and imaginary parts of φ are solutions to Beltrami's equations

$$\begin{aligned} \xi_x &= \mathcal{M}(c\eta_y + b\eta_x) \\ -\xi_y &= \mathcal{M}(a\eta_x + b\eta_y) \end{aligned} \tag{2.1}$$

where a, b, c are functions of x and y with $a, c > 0$ and satisfy the equation $ac - b^2 = 1$ on D and $\mathcal{M}$ is the dilation of the mapping.

We only consider the special case where $a = c = 1$ and $b = 0$. Then (2.1) reduces to

$$\begin{aligned} \xi_x &= \mathcal{M}\eta_y \\ -\xi_y &= \mathcal{M}\eta_x. \end{aligned} \tag{2.2}$$

This system is just the Cauchy-Riemann equations, except for the stretching factor $\mathcal{M}$. Under these conditions, we see that the mapping is orthogonal and satisfies Laplace's equation:

$$\Delta\varphi = 0.$$

The inverse mapping satisfies

$$\mathrm{g}_{22}\mathbf{r}_{\xi\xi} + \mathrm{g}_{11}\mathbf{r}_{\eta\eta} = 0,$$

where $\mathbf{r} = \big(x(\xi,\eta), y(\xi,\eta)\big)$, $\mathrm{g}_{11} = \mathbf{r}_\xi \cdot \mathbf{r}_\xi$, and $\mathrm{g}_{22} = \mathbf{r}_\eta \cdot \mathbf{r}_\eta$.[2] This system is then discretized to be

$$\mathbf{r}_{i,j} = \frac{\omega^2_{i+1,j}\mathbf{r}_{i+1,j} + \omega^2_{i-1,j}\mathbf{r}_{i-1,j} + \omega^2_{i,j+1}\mathbf{r}_{i,j+1} + \omega^2_{i,j-1}\mathbf{r}_{i,j-1}}{\omega^2_{i+1,j} + \omega^2_{i-1,j} + \omega^2_{i,j+1} + \omega^2_{i,j-1}}, \tag{2.3}$$

where the weights $\omega_{i+1,j} = \sqrt{\mathrm{g}_{22}}$, $\omega_{i-1,j} = \sqrt{\mathrm{g}_{22}}$, $\omega_{i,j+1} = \sqrt{\mathrm{g}_{11}}$, and $\omega_{i,j-1} = \sqrt{\mathrm{g}_{11}}$.

A smoothing algorithm based on (2.3) is then implemented using Gauss-Seidel relaxations. Nodes are relaxed in sequential order using (2.3), and each new node location is immediately incorporated in subsequent relaxations. After a sufficient number of Gauss-Seidel sweeps, (2.3) is approximately satisfied, and the scheme is deemed to have converged.

3. GENERALIZATION OF ELLIPTIC SMOOTHING TO UNSTRUCTURED GRIDS

It is now desired to generalize (2.3) to the case where we have a 2-dimensional *unstructured* mesh. Hence, we do not assume a quadrilateral element shape or any regular mesh connectivity. Typically in such a mesh, we are dealing with triangular elements, but we are not restricting ourselves to this case.

For a node in such an unstructured mesh, list the neighbours p of in counterclockwise order $\{p_1, p_2, \ldots, p_{\deg(q)}\}$. (The neighbours of p are those nodes which share an edge with p.) Consider the following smoothing scheme:

$$\mathbf{r}_q = \frac{\sum_{k=1}^{\deg(q)} (\ p_{k-1}, p_{k+1})^2 \mathbf{r}_{p_k}}{\sum_{k=1}^{\deg(q)} (\ p_{k-1}, p_{k+1})^2}. \tag{3.1}$$

Here, $_{p_{k-1},p_{k+1}}$ refers to the distance between nodes p_{k-1} and p_{k+1}, and the subscripts "$k-1$" and "$k+1$" are evaluated *modulo* deg( ). (See Figure 2.)

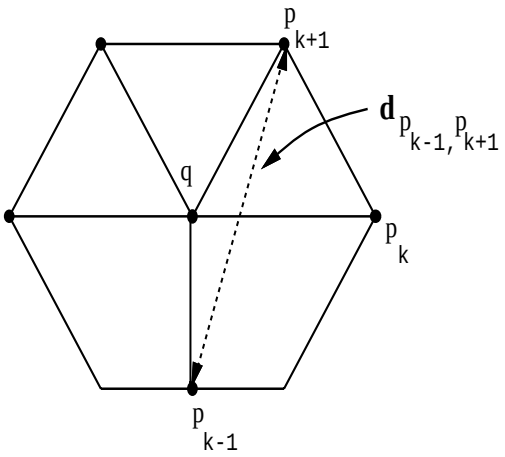

Figure 2. Distance used for weight of p_k in the relaxation of node in an unstructured grid.

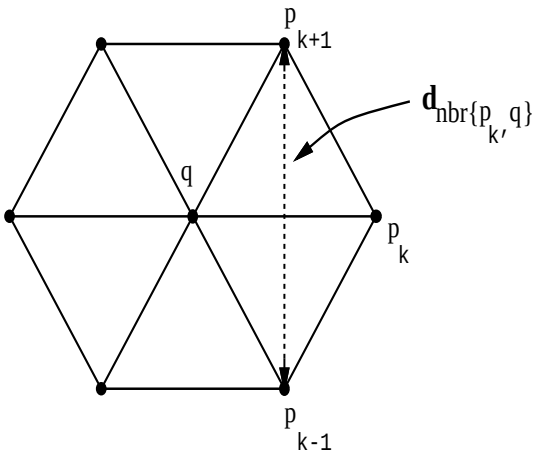

Figure 3. In a *triangular* unstructured grid, distance used for weight of p_k in the relaxation of node equals that for in the relaxation of node p_k.

Thus $\mathbf{r}_q$ is taken to be the weighted sum of the positions of the neighbours, and the weight for $\mathbf{r}_{p_k}$ is taken to be the square of the distance between the neighbours that come immediately before and after p_k in the listing of neighbours of . In the case of triangular unstructured grids, p_{k-1} and p_{k+1} have the property that they are the *two mutual neighbours* of and p_k. Then (3.1) is more naturally written as

$$\mathbf{r}_q = \frac{\sum_p (\ _{\mathrm{nbr}\{p,q\}})^2 \mathbf{r}_p}{\sum_p (\ _{\mathrm{nbr}\{p,q\}})^2}, \tag{3.2}$$

where $_{\mathrm{nbr}\{p,q\}}$ denotes the distance between the two mutual neighbours of nodes p and , and the sum is taken over all neighbours p of . (See Figure 3.)

We now claim that this scheme is identical to (2.3) in the special case of *structured* quadrilateral meshes. Indeed, observe that for the node at $\mathbf{r}_{i,j}$ in (2.3), the neighbours in counterclockwise order are $(i+1,j),(i,j+1),(i-1,j)$, and $(i,j-1)$. Now in the notation of (3.1), let $= (i,j)$ and consider $p_1 = (i+1,j)$. Then,

$$\begin{aligned} _{p_4,p_2} &= \text{distance between } \mathbf{r}_{i,j-1} \text{ and } \mathbf{r}_{i,j+1} \\ &= 2|\mathbf{r}_\eta| \\ &= 2\omega_{i+1,j}. \end{aligned}$$

Similarly, we find that

$$p_1,p_3 = 2\omega_{i,j+1},$$

$$p_2,p_4 = 2\omega_{i-1,j},$$

$$p_3,p_1 = 2\omega_{i,j-1},$$

and so all the unnormalized weights are identical to within a factor of 2^2, and hence the schemes are identical after normalization of the weights.

Equations (3.1) or (3.2) represent a generalization of elliptic smoothing to unstructured meshes. Note that if we had restricted ourselves to using merely a *conformal* mapping, then we would have had (2.2) with $\mathcal{M} = 1$. In this case, it is clear that we would have been led to (3.1) or (3.2) with the weights all set equal, which is the usual Laplacian smoothing scheme.

What we have *not* exhibited in our generalization is a global quasiconformal mapping, but that would be a daunting task, given the fact that the mesh connectivity is completely arbitrary. Also, our generalization is certainly not the only one possible. What we *do* exhibit in our generalization is the essential feature of the structured case algorithm: distance (squared) weighting, with the distance measured in a "transverse" direction. Hence it is not surprising that ESUG works in practice; we will see in the next section the superior ability of ESUG to diffuse points into an anisotropic domain. An added advantage of distance weighting is that the scheme is then naturally generalizable to solution adaption, as will be seen in Section 6.

4. COMPARISON OF ESUG WITH LAPLACIAN SMOOTHING IN AN ANISOTROPIC DOMAIN

In Figure 4, we consider a rectangle with 4:1 aspect ratio where we have purposely deposited a "source" of points in the middle. (The "strange" triangulation results from the fact that this grid was obtained by taking a section of a 3D tetrahedral mesh.) In Figures 5 and 6, we compare the effects of ESUG versus Laplacian smoothing. Clearly, the dense source of points in the middle has diffused far more in ESUG than in Laplacian smoothing. In the ESUG case, we see that the boundary triangles closest to the source of nodes have been allowed to deform in an appropriate anisotropic fashion, thus allowing the isotropic source of points to expand more than in the Laplacian case. In contrast, the boundary triangles nearest the middle in the Laplacian case are more "rigid" and expansion of the source of points is retarded.

Next we consider the effect of a sequence of smoothings and Lawson flips on these meshes. Lawson flips break the connectivity of the mesh and establish a Delaunay triangulation which is a common requirement for computation.[4] One might speculate that a repeated sequence of smoothings and Lawson flips would produce a uniform Delaunay

mesh. In Figure 7, we have subjected our initial grid to an alternating sequence of ESUG and Lawson flips, performing both procedures three times each. The result is a Delaunay mesh which appears as diffused as is possible given the fact that we have chosen not to move the points on the boundary.

In contrast, the same procedure with Laplacian smoothing substituted for ESUG yields Figure 8. Here the diffusion process has come to a standstill and does not appear to be enhanced by Lawson flipping. It is here quite apparent that the exclusive use of Laplacian smoothing along with changes of mesh connectivity may be *insufficient* to equilibrate node densities in many kinds of problem domains.

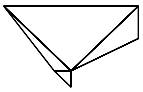

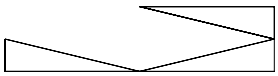

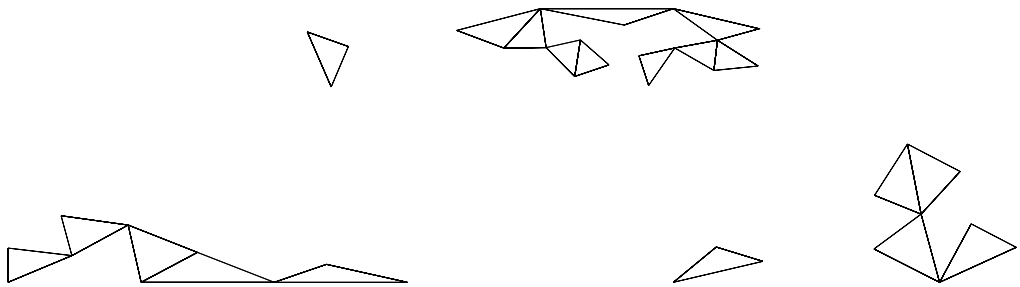

of smoothing schemes is obtained that are increasingly inhibited in the amount of node movement allowed. The following simple modification to (3.2) satisfies these criteria:

$$\mathbf{r}_q = \lambda \mathbf{r}_q^0 + (1-\lambda)\frac{\sum_p (\ _{\mathrm{nbr}\{p,q\}})^2 \mathbf{r}_p}{\sum_p (\ _{\mathrm{nbr}\{p,q\}})^2}, \tag{5.1}$$

Here, $\mathbf{r}_q^0$ corresponds to the *original* undisturbed position of node . In mathematical terms, we have constructed a simply homotopy between the identity map and our original smoothing scheme. Indeed, one could obtain such homotopies for any Gauss-Seidel node relaxation scheme by substituting those schemes into the right-hand side of (5.1). So, for example, Laplace smoothing would become

$$\mathbf{r}_q = \lambda \mathbf{r}_q^0 + (1-\lambda)\frac{\sum_p \mathbf{r}_p}{\deg(\ )}. \tag{5.2}$$

Not only is (5.1) a simple modification of (3.2), but we have found in practice that it retains the desirable element shape improving qualities of the original scheme. Although element areas are not *globally* equilibrated (for some nonzero value of λ), element areas are allowed to *locally* equilibrate—and this is exactly what is desired.

6. ADAPTIVE ELLIPTIC SMOOTHING FOR UNSTRUCTURED GRIDS

In many applications, it is desirable to smooth the mesh in such a fashion as to adapt it to some function defined over that mesh. Suppose the function $f(x,y)$ is the solution to a PDE, and it is desired to move nodes into regions where the gradient of f is large. (It can be argued that in many cases it is in regions of *curvature* of f that high node density is desired[5], but this is essentially equivalent to packing grid points into regions where the functions $g = \frac{\partial f}{\partial x}$ and $h = \frac{\partial f}{\partial y}$ have large gradients.)

Our original ESUG scheme can be readily turned into a scheme for adapting to ∇f by recognizing that the $_{\mathrm{nbr}\{p,q\}}$ in (3.2) have the dimensions of distance. These distances can readily be "warped" to force the scheme to adapt to the gradients of f. Indeed, if one considers the distance from a point p_k to a point $p_{k'}$ to be the distance along the *graph* of f:

$$(\ _{p_k,p_{k'}})^2 = (x_{p_k} - x_{p_{k'}})^2 + (y_{p_k} - y_{p_{k'}})^2 + (f_{p_k} - f_{p_{k'}})^2, \tag{6.1}$$

then our elliptic scheme is being essentially performed *on* the graph of f (i.e., on the surface $z = f(x,y)$). Hence, if element areas are equidistributed on this surface, the effect of this will be to move grid points into the gradient regions (see Figure 9).

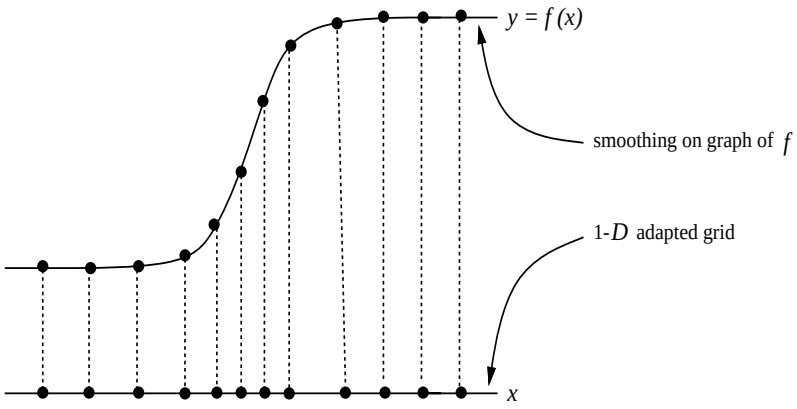

Figure 9. 1-D Simplification of Adaptive Smoothing Strategy.
In reality f is bivariate and we produce a 2-D adapted grid.

cannot occur for either scheme when the surrounding neighbours form a convex polygon. However, when the neighbours of a node form a nonconvex polygon, both methods are prone to spillover.

To prevent spillover, we limit movement at each Gauss-Seidel node relaxation by multiplying the node displacement prescribed by (3.1), (3.2), or (5.1) by a damping factor which insures that no triangle suffers more than a 25% loss in area in any single node relaxation. (If no triangle would suffer such a loss, the damping factor is simply unity.) However, this damping only becomes significant in some cases of smoothing near nonconvex boundaries or adaptive smoothing to "challenging" functions with extreme changes in gradient.

8. MOSFET SEMICONDUCTOR EXAMPLE

In Figure 10 we show an initial grid taken from an actual MOSFET semiconductor application. In Figure 11 we show a perspective view of a doping function $f_0(x,y)$ to which we wish to adapt our grid. (As can be seen, $f_0(x,y)$ is piecewise linear and contains extremely sharp gradients. The fine grid in this figure is used only for the definition of the function and is *not* the grid that we are trying to adapt.) Adaptive smoothing is to be performed on the shaded portion Ω of the grid in Figure 10, which corresponds to most of the Silicon substrate portion of the device.

In Figure 12 we show the effects of initially running the adaptive smoothing algorithm [(3.1) and (6.1)] on the grid in Figure 10. Some adaption to the steep gradient is observed. However we observe that better adaption can be obtained by using an alternating sequence of adaptive smoothing followed by Lawson flips, followed by more adaptive smoothing, etc. In Figure 13 we show the results of 10 adaptive smoothings, alternated with 10 rounds of Lawson flips. The flips cause topological changes that ultimately allow for a better adapted mesh. In fact, we note that Figure 10 and Figure 12 are topologically equivalent, and this topology is clearly not the best one for adapting to the function of Figure 11. This is indicated by the unnecessarily stretched triangles in Figure 12. In Figure 13 we see that Lawson flips have eliminated the unnecessarily stretched triangles, and have allowed more of the grid to move into the challenging steep gradient region.

A final technical note pertaining to the grid in Figure 13 is that the last stage of Lawson flipping also included the insertion of a small number of nodes (7) on the boundary of the smoothed region. This is to eliminate obtuse boundary-facing angles, which is a requirement of our finite volume solver. In general, obtuse boundary-facing angles (those angles opposite a boundary edge) cannot all be eliminated by Lawson flips of the interior edges. Hence the last stage of Lawson flipping actually consists of an alternating sequence of flips and boundary point insertions where necessary.

Next we try the alternate approach of using adaptive refinement followed by non-adaptive smoothing. In Figure 14 we have refined the initial grid in the shaded region Ω where the doping function has the large gradient. (More precisely, the refined grid is

actually a section of a tetrahedral grid which has had its edges refined a couple of times in the high gradient region.) Unfortunately the refinement has produced poorly-shaped triangles in this critical region, exhibiting a poor distribution of triangle areas. Also, due to asymmetry in the connectivity of the piecewise linear doping function, the refinement exhibits marked asymmetry. Then in Figure 15 we show the results of applying the plain (uncontrolled, non-adaptive) elliptic smoothing algorithm (3.2) on the shaded portion of Figure 14. The effect is that indeed the triangle areas are well equilibrated. However the regions of refinement have been oversmoothed, reducing the node density in these critical regions. Finally, in Figure 16, we show the results of our *controlled* elliptic smoothing algorithm (5.1). Here we have chosen $\lambda = \frac{1}{2}$. As can be seen, the node density in the critical regions is preserved but, as in Figure 15, triangle shape, area distribution, and symmetry are greatly improved. Finally we note that to make this grid suitable for finite volume computation, we should again follow smoothing by a round of Lawson flips with possible boundary point insertions.

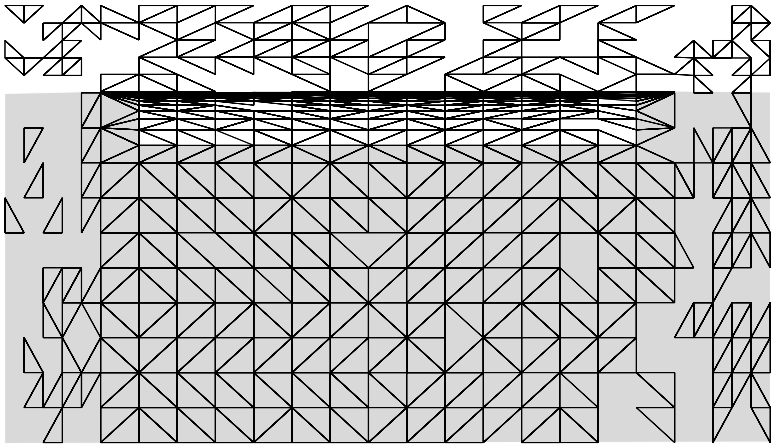

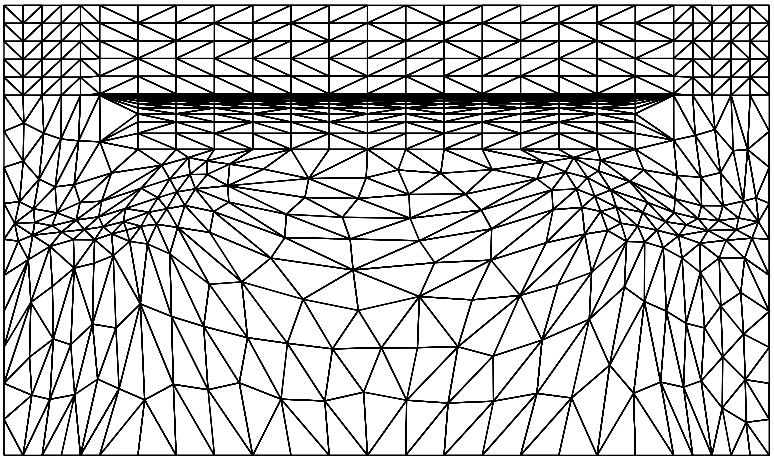

Figure 12. Grid after adaptive elliptic smoothing.

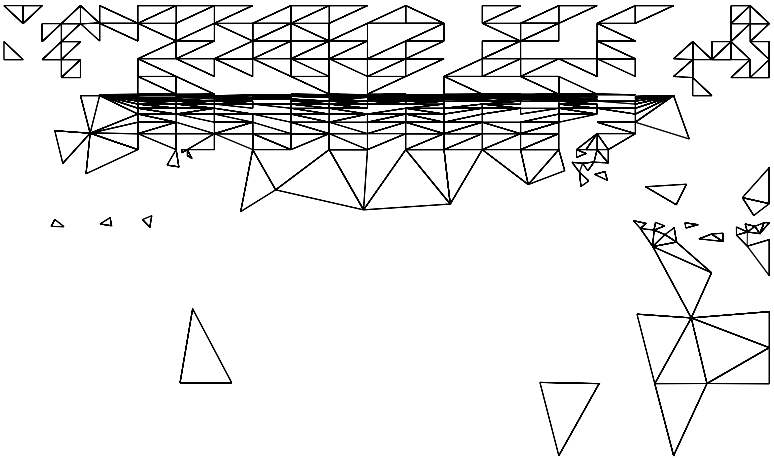

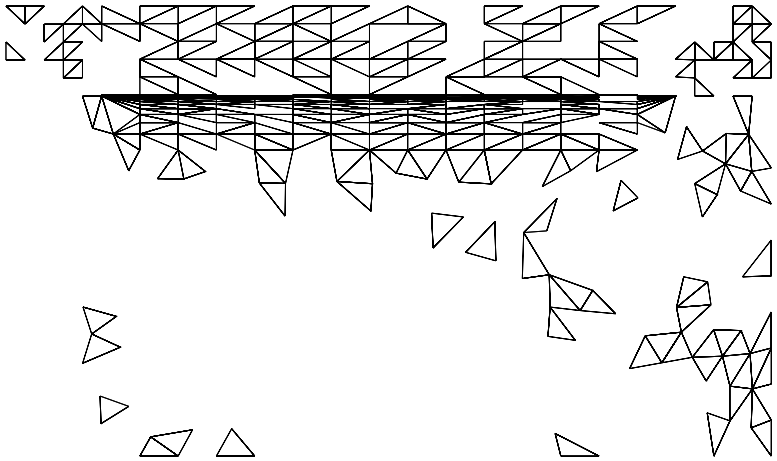

Figure	$\|\|e\|\|_\infty$	Figure	$\|\|e\|\|_\infty$
10	0.770	14	0.505
12	0.656	15	0.540
13	0.409	16	0.446

Table 1. Comparisons of smoothing/swapping/refinement schemes in the infinity norm.

We see here that smoothing alone (Figure 12) is not very effective in reducing the error. The best result is obtained in Figure 13, which represents a combination of smoothing and swapping. Adaptive refinement without smoothing (Figure 14) is also effective in reducing the error. As expected, unconstrained smoothing after adaptive refinement (Figure 15) undoes some of the benefits of refinement, but constrained smoothing after adaptive refinement (Figure 16) further reduces the error.

9. CONCLUSIONS

In this paper we have presented a scheme ESUG for smoothing an unstructured grid which, in its simplest form, is nearly as easy to implement as the standard Laplacian smoothing scheme.

The simplest "uncontrolled", non-adaptive form of the scheme shows a superior ability to equilibrate node densities and triangle areas in anisotropic domains than the standard Laplacian smoothing scheme. Combining ESUG with Lawson flipping further enhances the ability of the scheme to move the nodes. In fact non-adaptive ESUG with Lawson flipping has recently been used to equilibrate node densities in anisotropic geologic strata.[8] Thus we conclude that ESUG combined with Lawson flipping can be a useful tool for generating smooth grids in problem domains with complex shape.

For purposes of adapting a grid to capture the behaviour of an objective function, we developed two additional enhancements—"controlled" and "adaptive" ESUG. On a realistic MOSFET semiconductor problem we found that the combination of adaptive ESUG with Lawson flips provided a considerable reduction in error, while adaptive ESUG alone was not as effective. Adaptive refinement alone produced a good reduction in error, and the error could be reduced further using "controlled" ESUG.

We conclude that for purposes of adapting a grid to an objective function, the appropriateness of ESUG is problem dependent. If the cost of computation per node is inexpensive, then adaptive or uniform refinement without smoothing is straightforward and probably adequate. If the cost of computation per node is relatively expensive, then an ESUG adaptively smoothed mesh can provide increased accuracy comparable to that afforded by refinement, without increasing the number of nodes.

REFERENCES

1. C. W. Mastin, 'Elliptic Grid Generation and Conformal Mapping', in *Mathematical Aspects of Numerical Grid Generation*, edited by Jose E. Castillo, SIAM, 1991.

2. C.W. Mastin and J.F. Thompson, 'Quasiconformal Mappings and Grid Generation', *SIAM J. Sci. Stat. Comput.* **5**, 305–310 (1984).

3. A. M. Winslow, 'Numerical Solution of the Quasilinear Poisson Equation in a Nonuniform Triangle Mesh', *J. Comput. Phys.* **2**, 149–172 (1967).

4. C. L. Lawson, 'Software for C^1 Surface Interpolation', in *Mathematical Software III*, edited by John R. Rice, Academic Press, 1977.

5. R. E. Bank and R. K. Smith, 'Mesh smoothing using a posteriori error estimates', *SIAM J. Sci. Comp.* (to appear).

6. M. G. Vallet, F. Hecht, and B. Mantel, 'Anisotropic Control of Mesh Generation based upon a Voronoi Type Method', in *Numerical Grid Generation in Computational Fluid Dynamics and Related Fields*, edited by A. S. Arcilla et al., North-Holland, 1991.

7. D. A. Field, 'Laplacian smoothing and Delaunay triangulation', *Commun. Appl. Numer. Methods* **4**, 709–712 (1988).

8. C. W. Gable, H. E. Trease, and T. A. Cherry, 'Geological Applications of Automatic Grid Generation Tools for Finite Elements Applied to Porous Flow Modeling', *Proceedings of the Fifth International Conference on Numerical Grid Generation in Computational Fluid Dynamics and Related Fields*, edited by B. K. Soni et al., ERC-MSU Press, 1996.